Research paper

Cerebrospinal fluid: Profiling and fragmentation of gangliosides by ion mobility mass spectrometry

Mirela Sarbu [a], Shannon Raab [b], Lucas Henderson [b], Dragana Fabris [c], Zeljka Vukelic [c], David E. Clemmer [b], Alina D. Zamfir [a, d, *]

[a] National Institute for Research and Development in Electrochemistry and Condensed Matter, Timisoara, Romania
[b] Department of Chemistry, Indiana University, Bloomington, IN, USA
[c] Department of Chemistry and Biochemistry, University of Zagreb, School of Medicine, Zagreb, Croatia
[d] "Aurel Vlaicu" University of Arad, Arad, Romania

ABSTRACT

The proximity of cerebrospinal fluid (CSF) with the brain, its permanent renewal and better availability for research than tissue biopsies, as well as ganglioside (GG) shedding from brain to CSF, impelled lately the development of protocols for the characterization of these glycoconjugates and discovery of central nervous system biomarkers expressed in CSF. Currently, the investigation of CSF gangliosides is focused on concentration measurements of the predominant classes and much less on their profiling and structural analysis.

Since we have demonstrated recently the high performance of ion mobility separation mass spectrometry (IMS MS) for compositional and structural determination of human brain GGs, in the present study we have implemented for the first time IMS MS for the exploration of human CSF gangliosidome, in order to generate the first robust mass spectral database of CSF gangliosides. IMS MS separation and screening revealed 113 distinct GG species in CSF, having similar compositions to the species detected in human brain. In comparison with the brain tissue, we have discovered in CSF several components containing fatty acids with odd number of carbon atoms and/or short glycan chains. By tandem MS (MS/MS) we have further analyzed the structure of GD3(d18:1/18:0) and GD2(d18:1/18:0), two glycoforms exhibiting short carbohydrate chains found in CSF, but discovered and characterized previously in brain as well. According to the present results, human CSF and brain show a similar ganglioside pattern, a finding that might be useful in clinical research focused on discovery of ganglioside species associated to neurodegenerative diseases and brain tumors.

1. Introduction

Due to its constant physical contact with the brain and spinal cord and its daily renewal [1], cerebrospinal fluid (CSF) is a body fluid, which reflects the pathophysiological state of the brain. In the last decades, CSF started to represent an increasingly sought matrix for the detection and characterization of central nervous system (CNS) disorders. Although the existence of a clear, colorless fluid that surrounds the brain was known since the time of Hippocrates [2], the first descriptions of CSF production-absorption cycle belonged to Cushing in 1914 [3], and in 1919 to Dandy [4]. Produced in the choroid plexuses of the ventricles of the brain, and absorbed in the arachnoid granulations, containing mainly water (99%), and in a lesser extent (1%) proteins, glucose, neurotransmitters and electrolytes, the CSF has multiple functions [5,6]. CSF is designed to i) protect the brain tissue from trauma when jolted or hit by acting as a shock absorber; ii) offer immunological protection of the CNS; iii) transport nutrients, hormones, drugs and clean CNS from different metabolic waste, by purging them via the blood-brain barrier. Besides, CSF acts as a cushion for the brain, ensuring the buoyancy of the brain, preventing therefore the cut off blood supply and the death of neurons in the lower part of the brain [7], by reducing its normal weight from 1400 to 1500 g, to about 25—50 g

* Corresponding author. Plautius Andronescu Str. 1, RO-300224, Timisoara, Romania.
E-mail address: alina.zamfir@uav.ro (A.D. Zamfir).

when floating in CSF [1,8].

Nowadays, CSF collected by lumbar puncture is routinely examined to diagnose or to further confirm an established diagnosis for a variety of CNS disorders, such as Alzheimer disease, Rett syndrome, GM1 gangliosidosis, HIV-1 infection [9—11]. Additionally to CSF color and pressure monitoring, the current investigation techniques enable the counting and identification of several markers. While elevated levels of white blood cells are specific for infections, such as meningitis, increased levels of red blood cells are characteristic for subarachnoid haemorrhage [12]; the type and nature of proteins in CSF may serve for the diagnosis of multiple sclerosis, paraneoplastic syndromes, neurosarcoidosis, etc. [1], while Aquaporin 4 antibody for autoimmune conditions [1]. Glucose, lipids, hormones, secreted growth factors, neurotransmitters, cytokines, morphogens, viruses, bacteria and microRNAs interfere in the production, absorption, and functions of CSF and may be used as markers of hydrocephaly, tumors, intraventricular hemorrhages and congenital webs [6,13—16].

An important class of molecules with vital biological roles, whose changes in concentration and composition could be also monitored in CSF, is represented by the gangliosides (GGs). GGs are sialic acidic-containing glycosphingolipids found in the outer plasma membrane in all human cells, with the lipid moiety rooted into the external surface of the membrane and the saccharide core covering the membrane. The expression of GGs was demonstrated to be cell type-specific. At the brain level, gangliosides are considered valuable markers as their expression has a topographical specificity and varies with brain development, maturation and aging, as well as in neurodegeneration and malignant transformation [17—21]. Highly concentrated, especially in the cerebral cortex, up to 1000 times more than in any other extra-neural organ [22], to a certain extent, GGs are released into the intercellular space through the normal cell surface turnover, known as "cell surface shedding" [23]. Since in the intercellular space CSF and the GGs released from brain come in direct contact, CSF is enriched with brain ganglioside species [24,25]. However, their concentration in CSF is highly reduced, up to only 0.3—0.5 nmol/mL [25—27]; hence, the extraction, quantification and analysis of GGs from CSF require high performance techniques, characterized by elevated sensitivity and resolution.

GGs in CSF were approached primarily for the quantification of GM1, GD1 and GD3 classes by immunostaining [25], high performance thin layer chromatography (HPTLC) with densitometry [28], microimmunoaffinity by using anti-cholera toxin-B subunit monoclonal antibody coupled with chromatography and sialidase hydrolysis [29,30] or radioassay [31]. The aforementioned methods exhibit a series of limitations, since: i) large sample amounts are required; ii) GG preparation and their analysis are rather laborious and time-consuming; and iii) these methods provide insufficient sensitivity, specificity and structural information.

Over the past few years, mass spectrometry (MS) used alone, or in combination with separation techniques provided qualitative and quantitative data, at high sensitivity, accuracy, resolution and reproducibility, helpful for the characterization of GG species and their structural and functional interactions [17,20,21,32]. Electrospray ionization (ESI), nanoESI, chip-based nanoESI, or matrix assisted laser/desorption ionization (MALDI) coupled with high performance mass analyzers, such as quadrupole time-of-flight (QTOF), ion trap (IT) and Orbitrap [30,33—39], were implemented for screening, structural and semi-quantitative analyses of GGs, especially of those expressed in healthy or diseased brain tissue [40].

Nowadays, ion mobility separation (IMS) represents one of the most advanced analytical systems for MS, which demonstrated a high potential in identification of GG components in highly complex mixtures extracted from brain tissue. By IMS, the ions are separated not just according to the differences in size, but also in analyte collision cross section. Thereby, IMS is able to provide an exhaustive separation of gangliosides, according to glycan chain, sialylation degree and ceramide composition. This particular feature of IMS MS makes possible the discrimination of GG isomers and isobars. Besides, there are several other advantages which recommend IMS as a modern method of choice in the investigation of complex ganglioside mixtures, such as: i) identification of low abundant ions, indistinguishable solely by MS; ii) incorporation within the MS instrument; iii) the method does not require either special solvents or sample preparation procedures prior to MS; iv) can function properly for high-throughput analyses. Combined with fragmentation techniques, IMS MS is capable of complex mixture separation, detection by MS and structural characterization in a single run.

ESI IMS MS studies on native GG extracts from normal human brain [21,41,42] revealed a much higher number of glycoforms, than ever reported before. Novel structures, characterized by a higher degree of sialylation and diversity of the ceramide composition, some of them bearing non-carbohydrate type of attachments, were for the first time discovered by IMS MS. All these data could be obtained by efficient separation according to the carbohydrate chain length and the number of sialic acid (Neu5Ac) residues.

Up to now, only a limited number of studies based on MS targeted the detection and quantification of GGs from CSF [25,32,43—45]. Based on the similarities between the profile of gangliosides in CSF and cerebellum [26,46—49], the earlier results support the concept of brain ganglioside shedding into CSF.

Presently, the investigation of GG profile in CSF represents an approach of choice for early diagnosis of CNS afflictions based on molecular fingerprints, for the following reasons: i) the vital role played by GGs in neuronal and brain development by cell adhesion, activation, proliferation, motility and growth mediation, the formation and stabilization of functional synapses and neural circuits; ii) the preceding observations related to the similarity of GG content in CSF and brain; iii) the restricted access to brain biopsies or tumor tissue specimens; in some cases there is availability only post-mortem; iv) the constant renewal of CSF; v) the imperative necessity for development of routine protocols able to detect biomarkers prior the symptoms to occur, allow permanent examination of the biochemical changes during disease progression/regression or to follow the treatment effectiveness, which can be achieved through CSF sampling and analysis.

In this context, in the present study, for the first time, the native ganglioside extract was screened in healthy human CSFs to offer the first overview on the GG pattern in this body fluid with a crucial role at the CNS level. Moreover, this study employed the mobility separation system, MS and collision induced dissociation (CID) MS/MS, a combination of simple, rapid and highly sensitivity techniques that proved earlier their capability for a reliable separation, mapping, and structural analysis of glycolipids and discovery of ganglioside biomarkers in brain tissue.

Using this platform, the screening experiments revealed a large number of glycoforms in normal human CSF, which are analogous to the species detected by IMS MS in normal human brain. The ion mobility system allowed the separation based on the carbohydrate chain length and the degree of sialylation and thus, the detection even of low abundant GGs. Moreover, the elevated degree of sialylation identified in CSF, specific to human brain as well, supports the previous data related to the similarity of ganglioside expression in CSF and brain. Additionally, the combination of IMS with tandem MS (MS/MS) by CID was applied to confirm the structure of two ganglioside molecules associated to normal human CSF, characterized by shorter glycan chains.

IMS MS data obtained here represent a first step in generating a CSF GG inventory, which further might be used for finding specific molecular fingerprints valuable for early diagnosis of CNS disorders.

2. Experimental

2.1. Cerebrospinal fluid sampling

The normal lumbar CSFs investigated here were obtained from adult individuals exhibiting no signs of tumors, demyelination, intracranial haemorrhage, congenital errors of lipid metabolism or acute inflammatory process of the CNS. The CSFs were sampled by the Clinical Hospital Centre Zagreb, Department for General Clinical Biochemistry and Diagnostics of CSF, Croatia. The lumbar puncture and CSF characterization were performed in order to exclude meningitis associated to the patients, during an epidemic episode. Following these investigations, all CSF samples were found normal.

Approximately 1 mL of CSF was collected per individual patient diagnosed as healthy, as a residual volume after clinical analysis. The residual volumes of CSF samples from 21 patients were pooled and the total volume of 21 mL of pooled sample was collected. Gangliosides were extracted from 21 mL of normal CSF, which was provided for scientific purposes. Permission for experiments with human material for scientific purposes was obtained from The Ethical Commission of the University of Zagreb, Croatia, under project no. 108120 by the Ministry of Science and Technology of the Republic of Croatia. All procedures on the human tissue and/or human body fluids were in agreement with the 1964 Helsinki declaration and its later amendments.

After biochemical examinations, CSF samples were centrifuged for 10 min at 6,000 rpm in a mini-centrifuge (Thermo Fisher Scientific, USA). The native CSF supernatants were further used for ganglioside extraction.

2.2. Gangliosides extraction and purification

Ganglioside extraction was performed according to the method of Svennerholm and Fredman [50], modified by Vukelić et al. [51]. Briefly, the available volume of the CSF sample (21 mL) was divided into 7 aliquots containing 3 mL of CSF that were used for ganglioside isolation and purification. The 3 mL aliquots were treated as a corresponding water (W) homogenates in the extraction procedure usually performed with 10% water homogenates prepared from tissue samples. Chloroform (C) and methanol (M) were added to the CSF sample in order to obtain a total volume ratio 1:2:0.75 (C/M/W, with "W" corresponding to CSF; therefore 4 mL of C, 8 mL of M and 3 mL of CSF). After lipid extraction (overnight at $+4^{\circ}$C), the mixture was centrifuged (25 min, 3000 rpm at $+4^{\circ}$C) and the clear supernatant was collected. The re-extraction was made on the precipitate using 1/4 of the total volume used for the first extraction (1:2:0.75; C/M/W, therefore 1 mL of C, 2 mL of M and 0.75 mL of water), and the procedure was repeated. Both supernatants were pooled and used for GG extraction by phase partition: for every 6 mL of C:M = 1:2 mixture in the pooled supernatant, 2.5 mL of water and 2.0 mL of C was added (therefore, 7 mL of W and 6 mL of C), gently mixed and left at room temperature until the complete separation of the phases. Clear upper phase (containing GGs) was collected and repartition was performed with lower phase by adding 1.0 mL of C, 1.0 mL of M and 0.7 mL of water for every 6.0 mL of the C:M = 1:2 mixture (therefore, 2.5 mL of C, 2.0 mL of M and 1.75 mL of W). After complete separation of the phases, upper phase was collected and pooled with the upper phase from the first partition and evaporated to dryness in air stream. The samples were divided into aliquots of smaller volumes to accelerate the evaporation procedure, which approximately took 1 h per sample aliquot. The temperature during evaporation was always below 37°C and centrifugation with cooling was performed in order to avoid potential GG degradation by high temperatures. To induce precipitation of residual proteins, the dried ganglioside extract (acquired from 3 mL of CSF) was dissolved in 1.0 mL of C/M/W (60:30:4.5, by vol.) and left for 12 h at -20 $^{\circ}$C. The precipitated protein complexes were removed by centrifugation (4000 rpm, 25 min at -5°C) and the clear supernatant was evaporated to dryness. Purification primarily from salts and possible residual protein-salt complexes was performed by gel-filtration on Sephadex-G25 Fine gel (Sigma-Aldrich). Dried GG extract was dissolved in 0.1 mL of C/M/W (60:30:4.5, by vol.), applied to the gel (total gel volume 1 mL) and eluted with 5 bed volumes (5 mL) of the mobile phase (C/M/W = 60:30:4.5, by vol.). The collected eluates were evaporated and pooled during evaporation into one sample, representing the extract from 21 mL of CSF. To preserve physiologically relevant alkali-labile species, no alkaline hydrolysis step was performed during purification. The entire ganglioside extract (from 21 mL of CSF) was dissolved in pure methanol and an aliquot of 1/30 of total GG extract was diluted in methanol to prepare a stock solution of 0.5 μg/mL (corresponding to approximately 700 μL of CSF). Prior to the experiments the stock solution was stored at -40 °C.

2.3. Ion mobility mass spectrometry

The ion mobility mass spectrometry experiments on CSF were conducted in negative ionization mode on a Synapt G2S mass spectrometer (Waters, Manchester, UK) equipped with nanoESI source. The Synapt G2S MS was interfaced to a PC computer running the Waters MassLynx (version V4.1, SCN 855) and Waters Driftscope (version V2.7) software for data acquisition and IMS data processing.

Uncoated borosilicate glass (ID: 1.2 mm, OD: 1.5 mm) was purchased from Sutter Instrument Co. (Novato, CA). The 10 cm long capillaries were pulled with a Sutter p-97 micropipette puller to produce electrospray capillaries with 10 μm tip sizes and taper lengths of 4 mm. An aliquot of the stock solution was prepared by diluting the stock solution (0.5 μg/mL) in methanol 300 times to yield a solution of 5 pmol/μL GG-SA concentration. 30 μL of the solution at 5 pmol/μL GG concentration were introduced into the back of a pulled emitter and a 0.25 mm platinum wire was inserted into the solution. The potential values applied to the platinum wire and the cone was thoroughly adjusted to achieve an efficient ionization of the components and a negligible in-source fragmentation. A sustained and consistent spray was obtained at 1.6 kV and 45 V potential for capillary and cone, respectively. The emitter was positioned onto a stage for alignment to the Synapt G2S instrument. Other conditions responsible for the ionization process were set as follows: source block temperature 100 °C, desolvation gas flow rate 800 L/h, desolvation temperature 150 °C.

Besides the size, charge, shape and apparent surface area, which are distinctive for each molecule and have a great influence on the separation process, the instrumental setup parameters, such as IM cell gas pressure, amplitude and travel velocities are also responsible for the drift velocity. To increase the GG separation, the IMS parameters were adjusted to 90 mL/min IMS gas flow, 650 m/s IMS wave velocity, 40 V IMS wave height. For the screening experiment, low-mass (LM) and high-mass (HM) resolution parameters were set at 18 and 15, respectively, while for CID tandem MS, both at 15. The fragmentation experiments were conducted in the transfer cell, which is situated after the mobility cell, as the discrimination of the parent ion isomers, if present, is provided. For high sequence ion

coverage, collision energies between 30 and 40 eV were applied. The sensitivity of the employed analytical method is evidenced by the reduced sample consumption. Hence, for the approximate sample concentration of 5 pmol/μL, 660 scans, acquired in 5 min for MS screening and 6 min for structural characterization by CID MS/MS, are equivalent with a consumption of 3.2 μL, which correspond to only 16 pmols of GGs from CSF.

2.4. Ganglioside abbreviation and assignment of the spectra

For assigning the gangliosides, the abbreviation system introduced by Svennerholm [52] and the recommendations of IUPAC-IUB Commission on Biochemical Nomenclature (IUPAC-IUB 1998) [53] were applied. Further, the assignment of the sugar backbone sequence ions generated subsequent the fragmentation experiment was conducted according to the nomenclature introduced by Domon and Costello [54] and revised by Costello et al. [55].

GA3 - II^3-LacCer; GM1 - II^3-α-Neu5Ac-Gg$_4$Cer; GM2 - II^3-α-Neu5Ac-Gg$_3$Cer; GM3 - II^3-α-Neu5Ac-LacCer; GM4 - II^3-α-Neu5Ac-GgCer; GD1 - II^3-α-(Neu5Ac)$_2$-Gg$_4$Cer; GD2 - II^3-α-(Neu5Ac)$_2$-Gg$_3$Cer; GD3 - II^3-α-(Neu5Ac)$_2$-LacCer; GT1 - II^3-α-(Neu5Ac)$_3$-Gg$_4$Cer; GT2 - II^3-α-(Neu5Ac)$_3$-Gg$_3$Cer; GT3 - II^3-α-(Neu5Ac)$_3$-LacCer, GT4 - II^3-α-(Neu5Ac)$_3$-GgCer; GQ1 - II^3-α-(Neu5Ac)$_4$-Gg$_4$Cer

3. Results and discussion

3.1. IMS MS screening

Thirty μL of ganglioside solution originating from CSF, at a concentration of 5 pmol/μL in methanol, were infused into Synapt G2S and submitted to negative ion mode nanoESI IMS MS after a thorough adjustment and optimization of the parameters.

The two-dimensional (2D) data set of CSF, generated after 5 min of signal acquisition is presented in Fig. 1a, while Fig. 1b and c illustrate the summed drift time distributions and mass spectrum obtained by integrating the 2D data across all *m/z* values and all drift times, respectively.

As also observed in the earlier studies conducted on this class of molecules [21,41,42], IMS reduces the spectral congestion by separating on a millisecond time-scale i) the chemical noise across a wide range of drift times that can be easily recognized as a broad, well-defined region; ii) the species into mobility groups, based on charge state, carbohydrate chain length and degree of sialylation (Fig. 1a). IMS method enhanced the detection of an elevated number of species, even of those low abundant, which could not be detected only by separation according to their mass to charge ratio. Considering that in CSF, the GGs are less expressed than in brain tissue [25–27], this feature is of major importance for decoding the complex mixtures in high-throughput mode.

The mass spectra of singly to quadruply charged GGs, illustrated in Fig. 2a,b,c,d, were generated by retaining the drift time for each region indicated in Fig. 1a and combining the chromatograms. An overview on the detected molecular ions, together with their putative structural assignment is provided in Table 1. For ion designation and postulation of structures, the exact mass calculation, the known biosynthesis pathway criteria and the previous knowledge upon this type of substrates [33–38,41,42,56,57], were considered.

Gangliosides are complex molecules, their variability being attributed not only to the carbohydrate chain length and degree of sialylation, but also to the length and unsaturation degree of both long-chain base (LCB) (sphingoid base) and fatty acid encompassed in the structure of the ceramide. Whereas glycoforms with C18-LCB, especially (d18:1/18:0) and (d18:1/20:0)-type of ceramides were found distributed in all tissues as main components, GGs with (d20:1/18:0), containing C20-LCB are specific

only for CNS [58,59], and their content increases throughout the life span [60–63]. In view of the C18-LCB ubiquity in brain, Table 1 lists the species with the more probable LCB; however, the incidence of GGs with C20-LCB cannot be excluded either and remains to be elucidated in a future study dedicated to the lipid structure of CSF gangliosides.

A detailed evaluation of Table 1 indicates that the spectra are dominated by singly-, doubly- and triply charged species and a rich molecular pattern characterized by a prominent diversity of the ceramide chains and the prevalence of biologically-relevant modifications. Following the differences in GG mobility through the buffer gas, 138 ions were detected and identified with an average mass accuracy of 6.5 ppm. These ions were assigned to 113 distinct ganglioside species. Of these, 76, mainly polysialylated belonging to GD, GT and GQ classes, were also found in different human brain regions following IMS MS [21,41,42], microfluidics-MS [17,64–66] or ultrahigh resolution MS [17,20,56,67] analyses. The rest of 37 structures from asialo-to tetrasialogangliosides, including two *O*−Ac were up to date solely detected in CSF, an aspect claiming for further research upon their role as CSF biomarkers.

More than 76% of the total 113 GGs identified here by (−) nanoESI IMS MS were found polysialylated which is similar with the percentage of the polysialylated ganglioside species (over 78%) detected in human brain using same approach [18,38,39]. This aspect substantiates the previous findings related to the similarity of GG expression in CSF and brain [26,46–49]. Thus, 40 *m/z* signals correspond to 34 GT-type species, 38 *m/z* signals correspond to 35 GD-type species, and 27 *m/z* signals are attributable to 17 GQ-type species, most of them having a tetrasaccharide sugar core in their composition (Fig. 3).

Moreover, by applying the same investigation technique, the polysialylated glycoforms in the GT1>GQ1>GD1 descending series were defining the adult human brain [41]. Such findings are in agreement with the previously published literature, according to which, the expression of GGs in CSF is similar to the one in brain and that GD1 and GT1 represent the main components in adult brain [25–27,68].

Additionally, 13 monosialylated structures (GM), characterized by shorter glycan chain could be detected. Interestingly, an elevated number of ions, more exactly 19 signals, were detected in Figs. 1a and 2a, and identified as corresponding to 14 asialo species of GA3-type bearing ceramides of variable constitution.

An elevated variation of fatty acid chain length, from 12 up to 26 carbon atoms in their composition, was also observed. Among the 113 species identified here, 17 were bearing fatty acids with odd number of carbon atoms, mainly C17 and C19, and no less than 22 GGs contained trihydroxylated sphingoid bases and/or hydroxylated fatty acids, over a half being GT1-type molecules.

The presence of *O*-fucosylation and *O*-acetylation attachments to biologically relevant species was previously associated to the advanced stages of tissue development [40,41], being influenced both by age and topographical factors [20]. Here, nine species were found modified by peripheral non-carbohydrate type of attachments. Of these, *O*-acetylation was predominant in GQ1 glycoforms, while *O*-fucosylation in GT1. Moreover, one *O*-Ac-GT1, one Fuc-GT3 were detected as well. According to preceding reports, human brain is likewise characterized by *O*−Ac and Fuc glycoforms in a larger extent [21,41,42]; from the total number of 31 *O*-acetylated and 43 *O*-fucosylated structures detected by (−) nanoESI IMS MS in different brain regions, more than a half were also identified in CSF. The observed variation could be correlated with the reduced expression of gangliosides in CSF, on the one hand, and the differences in the activity of fucosyl- and acetyltransferases on the other hand.
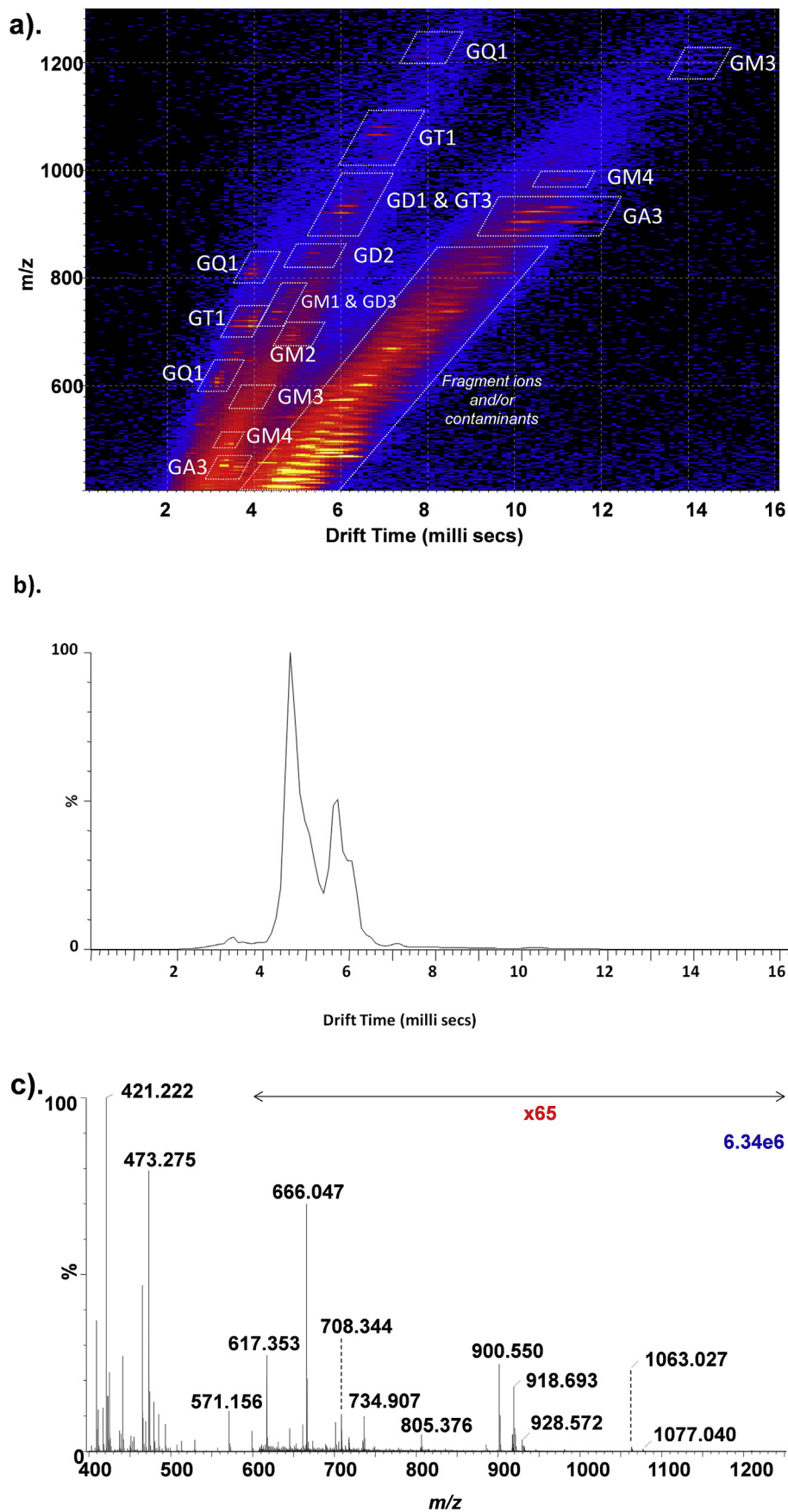
Fig. 1. (a) Driftscope display (drift time versus *m/z*) showing the total distribution of electrosprayed GG ions from CSF. The GG separation in the drift cell was according to the charge state (from singly to quadruply deprotonated species), carbohydrate chain length and the degree of sialylation; **(b)** the summed drift time distributions and **(c)** summed mass spectrum obtained by integrating the two-dimensional data across all *m/z* values and all drift times, respectively.
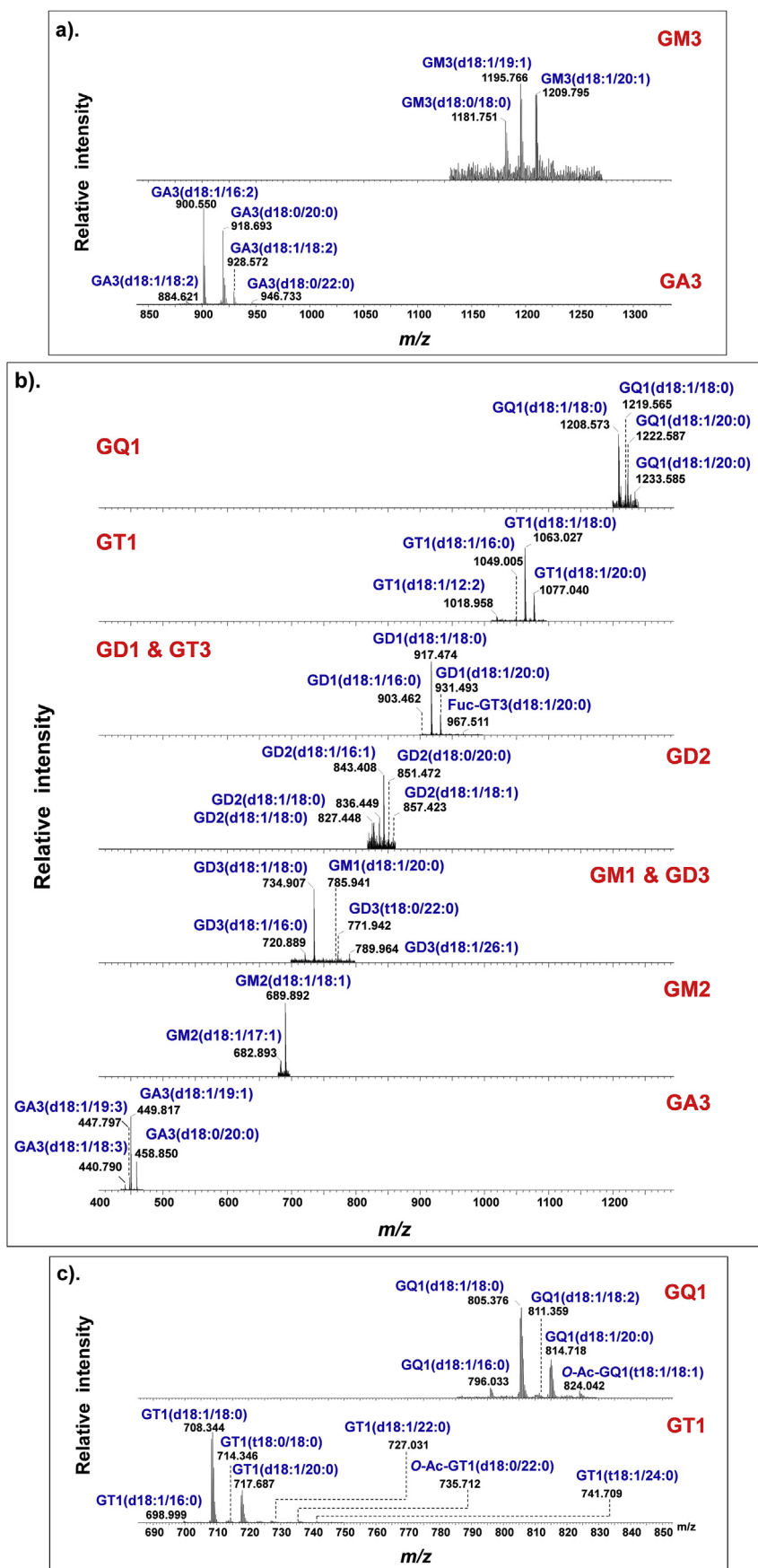
Fig. 2. Extracted mass spectra of (**a**) singly charged GA3 and GM3, (**b**) doubly charged GA3, GM2, GM1 & GD3, GD2, GD1 & GT3, GT1 and GQ1, (**c**) triply charged GT1 and GQ1 and (**d**) quadruply charged GQ1 from the corresponding areas indicated in Fig. 1a.

Table 1
Assignment of major ionic species detected in CSF by (−) nanoESI IMS MS.

No. Crt.	*m/z* exp.	*m/z* theor.	Mass accuracy (ppm)	Proposed structure*	Molecular ion
	433.782	433.788	13.9	GA3(d18:1/17:3)	[M − 2H]²⁻
	434.791	434.796	11.5	GA3(d18:1/17:2)	[M − 2H]²⁻
	438.775	438.780	11.4	GA3(d18:1/16:2)	[M − 3H +Na]²⁻
	439.781	439.788	15.9	GA3(d18:1/16:1)	[M − 3H +Na]²⁻
	440.790	440.796	13.6	GA3(d18:1/18:3)	[M − 2H]²⁻
	447.797	447.804	15.7	GA3(d18:1/19:3)	[M − 2H]²⁻
	449.817	449.820	6.7	GA3(d18:1/19:1)	[M − 2H]²⁻
	454.815	454.811	−8.8	GA3(d18:1/18:0)	[M − 3H +Na]²⁻
	456.833	456.828	−11.0	GA3(d18:1/20:1)	[M − 2H]²⁻
	458.850	458.844	−13.1	GA3(d18:0/20:0)	[M − 2H]²⁻
	490.289	490.294	10.2	GM4(d18:1/16:4)	[M − 2H]²⁻
	513.340	513.333	−13.6	GM4(d18:1/19:2)	[M − 2H]²⁻
	525.929	525.934	9.5	GT4(d18:1/17:3)	[M − 3H]³⁻
	578.319	578.328	15.6	GM3(d18:1/17:4)	[M − 2H]²⁻
	585.344	585.336	−13.7	GM3(d18:1/18:4)	[M − 2H]²⁻
	586.635	586.637	3.4	GT3(t18:0/18:0) and/or GT3(d18:0/h18:0)	[M-H₂O-3H]³⁻
	592.337	592.344	11.8	GM3(d18:1/19:4)	[M − 2H]²⁻
	596.276	596.272	−6.7	GQ1(d18:1/16:1)	[M − 4H]⁴⁻
	596.770	596.775	8.4	GQ1(d18:1/16:0)	[M − 4H]⁴⁻
	597.388	597.384	−6.7	GM3(d18:0/19:0)	[M − 2H]²⁻
	603.284	603.280	−6.6	GQ1(d18:1/18:1)	[M − 4H]⁴⁻
	603.778	603.783	8.3	GQ1(d18:1/18:0)	[M − 4H]⁴⁻
	607.280	607.278	−3.3	GQ1(t18:1/18:1) and/or GQ1(d18:1/h18:1)	[M − 4H]⁴⁻
	607.780	607.783	4.9	GQ1(t18:1/18:0) and/or GQ1(d18:1/h18:0)	[M − 4H]⁴⁻
	610.284	610.288	6.6	GQ1(d18:1/20:1)	[M − 4H]⁴⁻
	610.784	610.791	11.5	GQ1(d18:1/20:0)	[M − 4H]⁴⁻
	617.793	617.799	9.7	GQ1(d18:1/22:0)	[M − 4H]⁴⁻
	618.787	618.789	3.2	*O*-Ac-GQ1(t18:0/18:0) and/or *O*-Ac-GQ1(d18:0/h18:0)	[M − 4H]⁴⁻
	624.296	624.302	9.6	GQ1(d18:1/24:1)	[M − 4H]⁴⁻
	638.971	638.973	3.1	GT2(d18:1/15:2)	[M − 3H]³⁻
	643.649	643.644	−7.8	GT2(d18:0/14:0)	[M − 4H +Na]³⁻
	648.028	648.021	−10.8	GD1(d18:1/26:1)	[M − 3H]³⁻
	648.323	648.317	−9.3	GT2(d18:1/17:2)	[M − 3H]³⁻
	652.984	652.989	7.7	GT2(d18:1/18:2)	[M − 3H]³⁻
	657.656	657.661	7.6	GT2(d18:1/19:2)	[M − 3H]³⁻
	658.667	658.660	−10.6	Fuc-GD1(d18:1/18:2)	[M − 3H]³⁻
	659.001	659.005	6.1	GT2(d18:1/19:0)	[M − 3H]³⁻
	668.343	668.349	9.0	GT2(d18:1/21:0)	[M − 3H]³⁻
	681.883	681.883	0.0	GM2(d18:1/17:2)	[M − 2H]²⁻
	682.893	682.891	−2.9	GM2(d18:1/17:1)	[M − 2H]²⁻
	689.892	689.899	10.2	GM2(d18:1/18:1)	[M − 2H]²⁻
	698.999	699.004	7.2	GT1(d18:1/16:0)	[M − 3H]³⁻
	703.661	703.666	7.1	GT1(t18:1/16:1) and/or GT1(d18:1/h16:1)	[M − 3H]³⁻
	707.671	707.676	7.1	GT1(d18:1/18:1)	[M − 3H]³⁻
	708.344	708.348	5.6	GT1(d18:1/18:0)	[M − 3H]³⁻
	713.003	713.008	7.0	GT1(t18:1/18:1) and/or GT1(d18:1/h18:1)	[M − 3H]³⁻
	713.664	713.659	−7.0	GT1(d18:1/16:0)	[M − 5H +2Na]³⁻
	714.346	714.351	7.0	GT1(t18:0/18:0) and/or GT1(d18:0/h18:0)	[M − 3H]³⁻
	717.016	717.020	5.6	GT1(d18:1/20:1)	[M − 3H]³⁻
	717.687	717.692	7.0	GT1(d18:1/20:0)	[M − 3H]³⁻
	720.889	720.896	9.7	GD3(d18:1/16:0)	[M − 2H]²⁻
	722.348	722.352	5.5	GT1(t18:1/20:1) and/or GT1(d18:1/h20:1)	[M − 3H]³⁻
	723.031	723.025	−8.3	GT1(t18:1/20:0) and/or GT1(d18:1/h20:0)	[M − 3H]³⁻
	723.691	723.697	8.3	GT1(t18:0/20:0) and/or GT1(d18:0/h20:0)	[M − 3H]³⁻
	726.359	726.363	5.5	GT1(d18:1/22:1)	[M − 3H]³⁻
	727.031	727.036	6.9	GT1(d18:1/22:0)	[M − 3H]³⁻
	728.332	728.337	6.9	GT1(t18:1/20:3) and/or GT1(d18:1/h20:3)	[M-4H+Na]³⁻
	729.012	729.009	−4.1	GT1(t18:1/20:2) and/or GT1(d18:1/h20:2)	[M-4H+Na]³⁻
	732.364	732.369	6.8	GT1(t18:1/22:0) and/or GT1(d18:1/h22:0)	[M − 3H]³⁻
	733.045	733.041	−5.5	GT1(t18:0/22:0) and/or GT1(d18:0/h22:0)	[M − 3H]³⁻
	733.898	733.904	8.2	GD3(d18:1/18:1)	[M − 2H]²⁻
	734.907	734.912	6.8	GD3(d18:1/18:0)	[M − 2H]²⁻
	735.712	735.707	−6.8	*O*-Ac-GT1(d18:0/22:0)	[M-H₂O-3H]³⁻
	741.709	741.713	5.4	GT1(t18:1/24:0) and/or GT1(d18:1/h24:0)	[M − 3H]³⁻
	748.925	748.928	4.0	GD3(d18:1/20:0)	[M − 2H]²⁻
	762.937	762.943	7.9	GD3(d18:1/22:0)	[M − 2H]²⁻
	769.930	769.936	7.8	GD3(t18:1/22:1) and/or GD3(d18:1/h22:1)	[M − 2H]²⁻
	771.942	771.949	9.1	GD3(t18:0/22:0) and/or GD3(d18:0/h22:0)	[M − 2H]²⁻
	774.939	774.946	9.0	GD3(d18:1/24:2)	[M − 2H]²⁻
	775.949	775.951	2.6	GD3(d18:1/24:1)	[M − 2H]²⁻
	776.964	776.962	−2.6	GD3(d18:1/24:0)	[M − 2H]²⁻
	785.941	785.944	3.8	GM1(d18:1/20:0)	[M − 2H]²⁻

Table 1 (*continued*)

No. Crt.	m/z exp.	m/z theor.	Mass accuracy (ppm)	Proposed structure*	Molecular ion
	789.964	789.970	7.6	GD3(d18:1/26:1)	[M − 2H]²⁻
	796.033	796.036	3.8	GQ1(d18:1/16:0)	[M − 3H]³⁻
	804.706	804.708	2.5	GQ1(d18:1/18:1)	[M − 3H]³⁻
	805.376	805.377	1.2	GQ1(d18:1/18:0)	[M − 3H]³⁻
	810.038	810.041	3.7	*O*-Ac-GQ1(d18:1/16:0)	[M − 3H]³⁻
	810.706	810.713	8.6	*O*-Ac-GQ1(d18:0/16:0)	[M − 3H]³⁻
	811.359	811.365	7.4	GQ1(d18:1/18:2)	[M − 4H +Na]³⁻
	812.032	812.037	6.2	GQ1(d18:1/18:1)	[M − 4H +Na]³⁻
	814.057	814.053	−4.9	GQ1(d18:1/20:1)	[M − 3H]³⁻
	814.718	814.724	7.4	GQ1(d18:1/20:0)	[M − 3H]³⁻
	824.042	824.044	2.4	*O*-Ac-GQ1(t18:1/18:1) and/or *O*-Ac-GQ1(d18:1/h18:1)	[M − 3H]³⁻
	827.448	827.444	−4.8	GD2(d18:1/18:0)	[M-H₂O-2H]²⁻
	828.463	828.457	−7.2	GD2(d18:0/18:0)	[M-H₂O-2H]²⁻
	836.449	836.452	3.6	GD2(d18:1/18:0)	[M − 2H]²⁻
	843.408	843.413	5.9	GD2(d18:1/16:1)	[M − 4H +2Na]²⁻
	849.459	849.463	4.7	GD2(d18:1/20:1)	[M − 2H]²⁻
	850.466	850.471	5.9	GD2(d18:1/20:0)	[M − 2H]²⁻
	851.472	851.479	8.2	GD2(d18:0/20:0)	[M − 2H]²⁻
	857.423	857.429	7.0	GD2(d18:1/18:1)	[M − 4H +2Na]²⁻
	859.441	859.446	5.8	GD2(d18:1/20:2)	[M − 3H +Na]²⁻
	880.459	880.463	4.5	GT3(d18:1/18:0)	[M − 2H]²⁻
	882.594	882.600	6.8	GA3(d18:1/18:3)	[M − H]⁻
	884.621	884.616	−5.7	GA3(d18:1/18:2)	[M − H]⁻
	898.661	898.669	8.9	GA3(d18:1/20:0)	[M-H₂O-H]⁻
	900.550	900.548	−2.2	GA3(d18:1/16:2)	[M − 3H +2Na]⁻
	903.462	903.462	0.0	GD1(d18:1/16:0)	[M − 2H]²⁻
	907.464	907.468	4.4	GD1(d18:1/18:1)	[M-H₂O-2H]²⁻
	909.489	909.484	−5.5	GD1(d18:0/18:0)	[M-H₂O-2H]²⁻
	916.469	916.470	1.1	GD1(d18:1/18:1)	[M − 2H]²⁻
	916.686	916.680	−6.6	GA3(d18:1/20:0)	[M − H]⁻
	917.474	917.478	4.4	GD1(d18:1/18:0)	[M − 2H]²⁻
	918.693	918.696	3.3	GA3(d18:0/20:0)	[M − H]⁻
	924.469	924.471	2.2	GD1(t18:1/18:1) and/or GD1(d18:1/h18:1)	[M − 2H]²⁻
	925.475	925.479	4.3	GD1(t18:1/18:0) and/or GD1(d18:1/h18:0)	[M − 2H]²⁻
	926.488	926.487	−1.1	GD1(t18:0/18:0) and/or GD1(d18:0/h18:0)	[M − 2H]²⁻
	928.572	928.580	8.6	GA3(d18:1/18:2)	[M − 3H +2Na]⁻
	930.481	930.486	5.4	GD1(d18:1/20:1)	[M − 2H]²⁻
	931.493	931.494	1.1	GD1(d18:1/20:0)	[M − 2H]²⁻
	932.705	932.712	7.5	GA3(d18:0/21:0)	[M − H]⁻
	945.515	945.510	−5.3	GD1(d18:1/22:0)	[M − 2H]²⁻
	946.733	946.728	−5.3	GA3(d18:0/22:0)	[M − H]⁻
	956.506	958.514	−8.4	GD1(d18:1/24:3)	[M − 2H]²⁻
	958.506	956.498	8.4	GD1(d18:1/24:1)	[M − 2H]²⁻
	967.511	967.504	−7.2	Fuc-GT3(d18:1/20:0)	[M − 2H]²⁻
	981.590	981.595	5.1	GM4(d18:1/16:4)	[M − H]⁻
	988.488	988.492	4.0	Fuc-GD1(d18:1/18:2)	[M − 2H]²⁻
	989.495	989.499	4.0	Fuc-GD1(d18:1/18:1)	[M − 2H]²⁻
	990.501	990.507	6.1	Fuc-GD1(d18:1/18:0)	[M − 2H]²⁻
	991.992	991.985	−7.1	GT2(d18:1/18:1)	[M-3H+Na]²⁻
	1018.958	1018.963	4.9	GT1(d18:1/12:2)	[M − 2H]²⁻
	1019.966	1019.974	7.9	GT1(d18:1/12:1)	[M − 2H]²⁻
	1049.005	1049.010	4.8	GT1(d18:1/16:0)	[M − 2H]²⁻
	1062.014	1062.018	3.8	GT1(d18:1/18:1)	[M − 2H]²⁻
	1063.027	1063.026	−0.9	GT1(d18:1/18:0)	[M − 2H]²⁻
	1077.040	1077.042	1.9	GT1(d18:1/20:0)	[M − 2H]²⁻
	1091.053	1091.057	3.7	GT1(d18:1/22:0)	[M − 2H]²⁻
	1092.073	1092.068	−4.6	GT1(d18:0/22:0)	[M − 2H]²⁻
	1181.751	1181.759	6.8	GM3(d18:0/18:0)	[M − H]⁻
	1195.766	1195.775	7.5	GM3(d18:1/19:1)	[M − H]⁻
	1209.795	1209.791	−3.3	GM3(d18:1/20:1)	[M − H]⁻
	1208.573	1208.576	2.5	GQ1(d18:1/18:0)	[M − 2H]²⁻
	1209.580	1209.584	3.3	GQ1(d18:0/18:0)	[M − 2H]²⁻
	1212.565	1212.560	−4.1	GQ1(d18:1/17:0)	[M-3H+Na]²⁻
	1219.565	1219.567	1.6	GQ1(d18:1/18:0)	[M-3H+Na]²⁻
	1222.587	1222.589	1.6	GQ1(d18:1/20:0)	[M − 2H]²⁻
	1233.585	1233.583	−1.6	GQ1(d18:1/20:0)	[M-3H+Na]²⁻

3.2. IMS CID MS/MS structural characterization

Given the predominance in CSF of GG species characterized by shorter glycan chain, two doubly deprotonated molecules encompassing (d18:1/18:0) ceramide and two sialic acids linked to a di- and a trisaccharide core, were chosen for further detailed investigation by CID MS/MS. For the first fragmentation experiment, the ion detected at *m/z* 734.907 in Fig. 2b, displaying only one
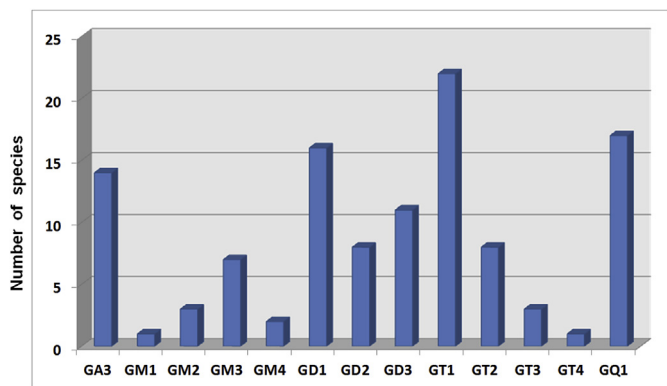
Fig. 3. Histogram plotting the number of the identified species in CSF of normal individuals, according to the composition of their glycan core and the sialylation degree.

mobility feature at 4.41 ms (*Inset* Fig. 4a), and assigned, according to mass calculation, to the doubly deprotonated GD3(d18:1/18:0), was isolated by setting LM to 15 and HM to 15 and submitted to low energy CID MS/MS in the negative ion mode.

The fragmentation spectrum obtained by combining 180 scans acquired for 3 min under variable collision energy within 30–40 eV range is presented in Fig. 4a. A scheme depicting the fragmentation pathway experienced by the precursor ion during the dissociation event is provided in Fig. 4b. As a result of the proper optimization of CID MS/MS parameters, a complete series of product ions, valuable for the assignment of both the carbohydrate and ceramide composition, were generated (Fig. 4a and b).

The sialylation status of the molecule is documented by the abundant B_1^- at *m/z* 290.019, C_1^- at *m/z* 308.030, the disialo element (Neu5Ac$_2$) as B_2^- at *m/z* 581.083, together with their counterparts Y_3^- at *m/z* 1179.622 and the asialo Y_2^- detected at *m/z* 888.532, respectively. On the other side, a series of diagnostic fragment ions, such as Y_0^- at *m/z* 564.443, U^- at *m/z* 283.195 and V^- at *m/z* 267.272 support the (d18:1/18:0) composition of the ceramide. Several other fragment ions, such as C_3^{2-} at *m/z* 380.011, C_3/CO_2^- at *m/z* 717.278, Z_1^- at *m/z* 708.485 and Y_1^- at *m/z* 726.501 corroborate together for the GD3(d18:1/18:0) composition of the fragmented ion. The spectrum in Fig. 4a also reveals that several double bond and internal cross-ring cleavages were induced, leading to the formation of $[^{2,4}A_4/C_1]^-$, $[Z_2/Z_1]^-$ and $[Y_2/Z_1]^-$ detected as signals at *m/z* 493.098, *m/z* 160.998, and *m/z* 179.003, respectively.

In the second CID MS/MS experiment, the ion at *m/z* 836.449 in Fig. 2b and assigned by mass calculation to GD2(d18:1/18:0) was submitted to structural characterization under identical experimental conditions. The resulted fragmentation spectrum is represented in Fig. 5a, while the fragmentation scheme of GD2(d18:1/18:0) is depicted in Fig. 5b. Exhibiting a quasi-similar constitution, with only a GalNAc residue in addition to the structure of the previously characterized GD3(d18:1/18:0), its fragmentation pattern was comparable. The MS/MS is dominated by typical B and Y-type fragment ions (Fig. 5a), as well. $B_{1\alpha}^-$ at *m/z* 290.019 with its counterpart $Y_{3\alpha}^-$ at *m/z* 1382.669, as well as $C_{1\alpha}^-$ at *m/z* 308.068 are indicative for the partial desialylation of the molecule, while the detachment of both Neu5Ac residues, leading to complete desialylation is documented by $B_{2\alpha}^-$, $B_{2\alpha}/CO_2^-$, $Y_{2\alpha}^-$ and $C_{2\alpha}^-$ at *m/z* 581.125, *m/z* 564.443, *m/z* 1091.611 and *m/z* 599.257, respectively. The detected Y series: $Y_{2\beta}^{2-}$ at *m/z* 734.880 generated by subsequent GalNAc detaching, Y_1^- at *m/z* 726.524 and Y_0^- at *m/z* 564.443 serves also for the confirmation of the reducing end.

In particular, Y_0^- at *m/z* 564.443 together with U^- at *m/z* 283.195

corresponding to the C18:0 fatty acid, validate (d18:1/18:0) ceramide composition. Likewise, $[^{2,4}A_4/C_{1\alpha}/C_{1\beta}]^-$, $[B_3/C_{2\alpha}]^-$, $[C_3/B_{1\beta}]^{2-}$ and $[Y_{2\alpha}/B_{1\beta}]^-$ at *m/z* 493.108, *m/z* 346.978, *m/z* 380.044 and *m/z* 888.558 formed by double bond and/or internal cross-ring cleavages are diagnostic for both nonreducing and reducing end.

4. Conclusions

In this work, the gangliosidome of normal human cerebrospinal fluid was investigated in details for the first time. Our strategy involved the combination of the most advanced separation technique, namely ion mobility separation, with high resolution MS, followed by CID MS/MS for separation, profiling and structural analysis in a single experiment of native gangliosides extracted from healthy CSFs.

Following a thorough optimization of both ionization and separation parameters, the results obtained here indicate along with a reduced spectral congestion, and a background chemical noise separation, the detection of highly rich glycoform pattern. The specific feature of GGs when separated by IMS, *i.e.* their division in classes based on the charge state, *m/z* ratio, carbohydrate chain length and degree of sialylation, was beneficial for the identification of no less than 113 species characterized by a high diversity of both glycan and ceramide chain lengths. Many of the structures were previously detected in human brain, while others were newly discovered, assigned with an average mass accuracy of 6.5 ppm and associated to the normal adult CSF. As revealed by IMS MS the ganglioside classes found in CSF are GT1>GQ1>GD1>GA3>GD3>GD2 = GT2>GM3>GM2 = GT3>GM4>GM1 = GT4, given here in descending order, based on their abundances. A relatively large number of species containing in their composition either fatty acids with odd number of carbon atoms, mainly C17 and C19, and/or short glycan moieties, were also identified. In addition, IMS MS evidenced four components modified by O-fucosylation and five by O-acetylation.

Overall, the data achieved by IMS MS screening experiments conducted in negative ion mode not only support the previously reported information gathered by quantitative studies upon the similarity of brain and CSF ganglioside composition, but also provide strong evidence upon the complexity of the GG pattern in this body fluid.

In the next stage of research, the structural confirmation of two biologically relevant glycoforms with shorter carbohydrate chain, a feature of CSF, was achieved by CID tandem MS at low collision energies in the transfer cell. Under optimized fragmentation conditions, using variable collision energy within 30–40 eV, a significant number of fragment ions diagnostic for both the glycan core and ceramide moiety of the postulated GD3(d18:1/18:0) and GD2(d18:1/18:0) were generated. Remarkably, the occurrence of a single mobility feature for each fragmented species discloses that only a single structural conformation exists for each case.

To our knowledge, this is the first systematic compositional and structural characterization of gangliosides in human cerebrospinal fluid and the first implementation of IMS MS and IMS CID MS/MS in human CSF ganglioside research. The valuable information acquired through the present study indicates on one side the efficacy of IMS MS technique for detection and structure elucidation of glycolipid species in biological fluids, where such molecules are in a reduced concentration, and, on the other side, provides the basis for advanced investigations targeting the discovery in CSF of ganglioside species associated to neurodegenerative diseases and brain tumors.
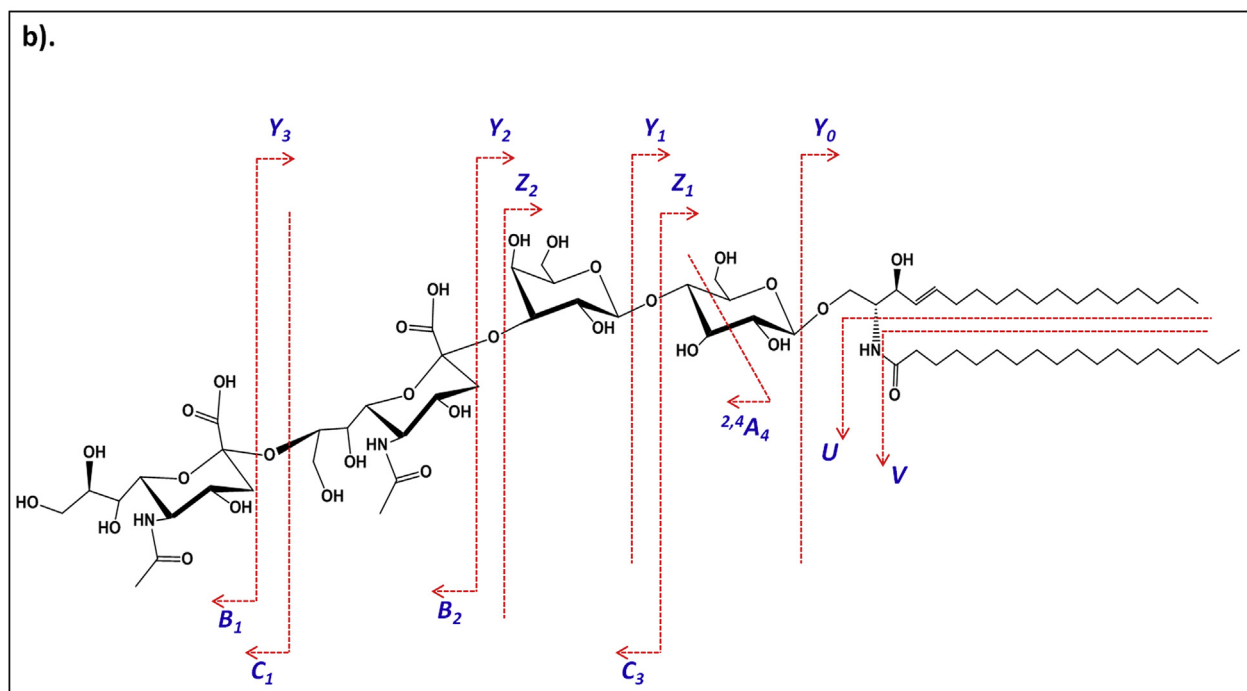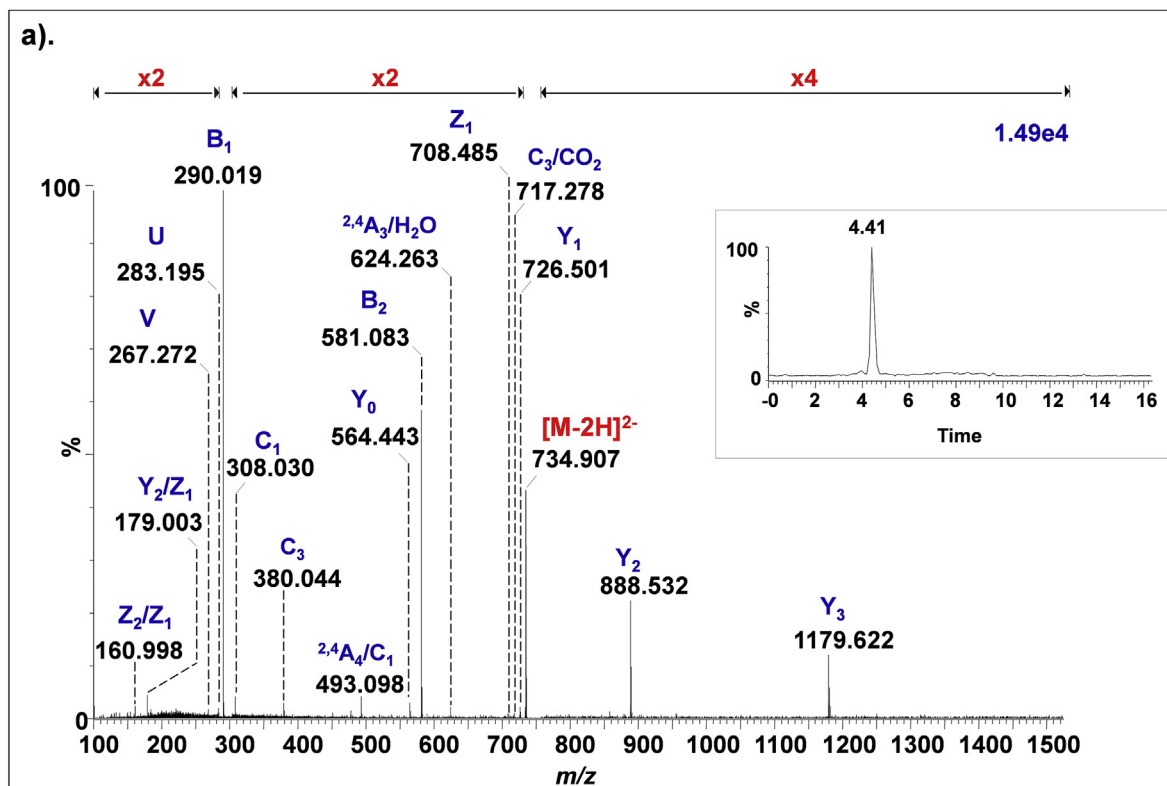
Fig. 4. (**a**) (−)nanoESI IMS CID MS/MS of the [M − 2H]²⁻ at *m/z* 734.907 corresponding to GD3(d18:1/18:0) species isolated and fragmented from CSF sample. *Inset*: drift time distribution for the ion at *m/z* 734.907 fragmented by CID. Cone voltage 45 V. Capillary voltage 1.6 kV. Acquisition 180 scans. CID at variable collision energy within 30—40 eV; (**b**) fragmentation scheme of GD3(d18:1/18:0).
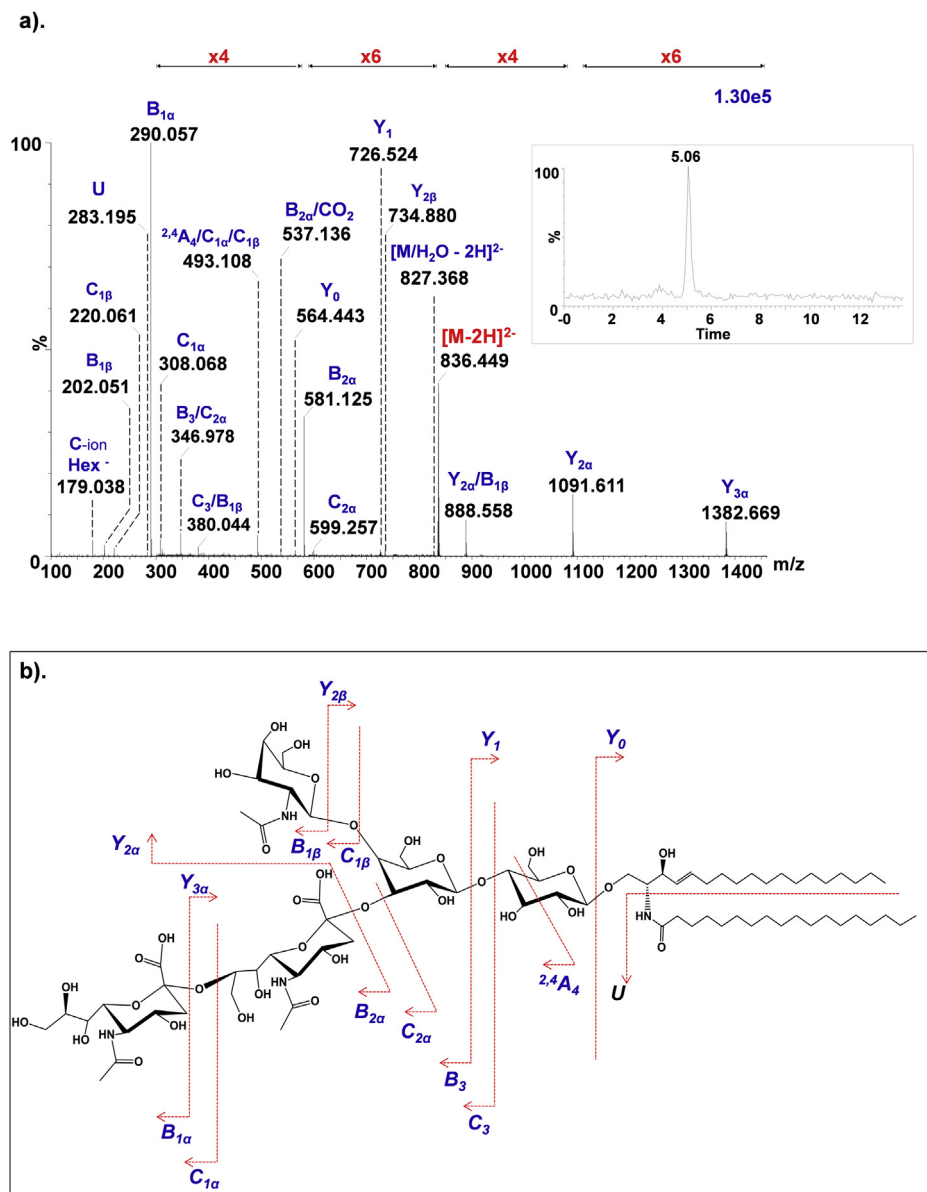
Fig. 5. (a) (−)nanoESI IMS CID MS/MS of the [M − 2H]²⁻ at *m/z* 836.449 corresponding to GD2(d18:1/18:0) species isolated and fragmented from CSF sample. *Inset*: drift time distribution for the ion at *m/z* 836.449 fragmented by CID. Cone voltage 45 V. Capillary voltage 1.6 kV. Acquisition 180 scans. CID at variable collision energy within 30—40 eV; **(b)** fragmentation scheme of GD2(d18:1/18:0).

Author contributions

M.S., D.F., Ž.V. and A.D.Z. conceived the original idea and planned the experiments. D.F. and Ž.V. collected the cerebrospinal fluid, extracted and purified the gangliosides. M.S., S.R. and L.H. carried out the IMS MS experiments and collected the data. M.S. and A.D.Z. analyzed the data. M.S., A.D.Z., D.E.C. and D.F. wrote the manuscript. A.D.Z. and D.E.C. supervised the project.

Declaration of competing interest

The authors declare that they have no known competing financial interests or personal relationships that could have appeared to influence the work reported in this paper.

Acknowledgements

This project was supported by the Romanian National Authority

References

[1] B.L.C. Wright, J.T.F. Lai, A.J. Sinclair, Cerebrospinal fluid and lumbar puncture: a practical review, J. Neurol. 259 (2012) 1530—1545.
[2] S.I. Hajdu, A note from history: discovery of the cerebrospinal fluid, Ann. Clin. Lab. Sci. 33 (2003) 334—346.
[3] H. Cushing, Studies on the cerebro-spinal fluid: I. Introduction, J. Media Res. 31 (1914) 1—19.
[4] W.E. Dandy, Experimental hydrocephalus, Ann. Surg. 70 (1919) 129—142.
[5] M. Bulat, M. Klarica, Recent insights into a new hydrodynamics of the cerebrospinal fluid, Brain Res. Rev. 65 (2011) 99—112.
[6] A.H. Khasawneh, R.J. Garling, C.A. Harris, Cerebrospinal fluid circulation: what do we know and how do we know it? Brain Circ 4 (2018) 14—18.
[7] K. Saladin, Anatomy and Physiology: the Unity of Form and Function, sixth ed., McGraw Hill, New York, 2012.
[8] C. Noback, N.L. Strominger, R.J. Demarest, D.A. Ruggiero, The Human Nervous System, sixth ed., Humana Press, New Jersey, 2005.

[9] A. Edén, D. Fuchs, L. Hagberg, S. Nilsson, S. Spudich, B. Svennerholm, R.W. Price, M. Gisslén, HIV-1 viral escape in cerebrospinal fluid of subjects on suppressive antiretroviral treatment, J. Infect. Dis. 202 (2010) 1819—1825.

[10] A.Y. Lekman, B.A. Hagberg, L.T. Svennerholm, Cerebrospinal fluid gangliosides in patients with Rett syndrome and infantile neuronal ceroid lipofuscinosis, Eur. J. Paediatr. Neurol. 3 (1999) 119—123.

[11] H. Satoh, T. Yamauchi, M. Yamasaki, Y. Maede, A. Yabuki, H.S. Chang, T. Asanuma, O. Yamato, Rapid detection of GM1 ganglioside in cerebrospinal fluid in dogs with GM1 gangliosidosis using matrix-assisted laser desorption ionization time-of-flight mass spectrometry, J. Vet. Diagn. Investig. 23 (2011) 1202—1207.

[12] D.A. Seehusen, M.M. Reeves, D.A. Fomin, CSF analysis, Am. Fam. Physician 68 (2003) 1103—1108.

[13] M. Vinchon, M. Baroncini, I. Delestret, Adult outcome of pediatric hydrocephalus, Childs Nerv Syst 28 (2012) 847—854.

[14] C. Johanson, N. Johanson, Merging transport data for choroid plexus with blood-brain barrier to model cns homeostasis and disease more effectively, CNS Neurol. Disord. - Drug Targets 15 (2016) 1151—1180.

[15] A.F. Huhmer, R.G. Biringer, H. Amato, A.N. Fonteh, M.G. Harrington, Protein analysis in human cerebrospinal fluid: physiological aspects, current progress and future challenges, Dis. Markers 22 (2006) 3—26.

[16] F. Deisenhammer, A. Bartos, R. Egg, N.E. Gilhus, G. Giovannoni, S. Rauer, F. Sellebjerg, E.T. Force, Guidelines on routine cerebrospinal fluid analysis. report from an EFNS task force, J. Neurol. 13 (2006) 913—922.

[17] A. Zamfir, Ž. Vukelić, L. Bindila, J. Peter-Katalinić, R. Almeida, A. Sterling, M. Allen, Fully-automated chip-based nanoelectrospray tandem mass spectrometry of gangliosides from human cerebellum, J. Am. Soc. Mass Spectrom. 15 (2004) 1649—1657.

[18] L. Svennerholm, K. Bostrom, P. Fredman, J.E. Mansson, B. Rosengren, B.M. Rynmark, Human brain gangliosides: developmental changes from early fetal stage to advanced age, Biochim. Biophys. Acta 1005 (1989) 109—117.

[19] T. Ariga, W.D. Jarvis, R.K. Yu, Role of sphingolipid-mediated cell death in neurodegenerative diseases, J. Lipid Res. 39 (1998) 1—16.

[20] M. Sarbu, L. Dehelean, C.V.A. Munteanu, Vukelić Ž, A.D. Zamfir, Assessment of ganglioside age-related and topographic specificity in human brain by orbitrap mass spectrometry, Anal. Biochem. 521 (2017) 40—54.

[21] M. Sarbu, Ž. Vukelić, D.E. Clemmer, A.D. Zamfir, Electrospray ionization ion mobility mass spectrometry provides novel insights into the pattern and activity of fetal hippocampus gangliosides, Biochimie 139 (2017) 81—94.

[22] L. Svennerholm, Structure and biology of cell membrane gangliosides, in: O. Ouchterlony, J. Holmgren (Eds.), Cholera and Related Diarrheas, Karger, Basel, 1980, p. 80.

[23] F. Doljanski, M. Kapeller, Cell surface shedding: the phenomenon and its possible significance, J. Theor. Biol. 62 (1976) 253—270.

[24] T. Milhorat, K. Hammock, Cerebrospinal fluid as reflection of internal milieu of brain, in: J.H. Wood (Ed.), Neurobiology of Cerebrospinal Fluid, Plenum Press, New York, 1983, p. 1.

[25] S. Ladisch, F. Chang, R. Li, P. Cogen, D. Johnson, Detection of medulloblastoma and astrocytoma-associated ganglioside GD3 in cerebrospinal fluid, Cancer Lett. 120 (1997) 71—78.

[26] R.W. Ledeen, R.K. Yu, Gangliosides of CSF and plasma: their relation to the nervous system, in: B.W. Volk, S.M. Aronson (Eds.), Sphingolipids, Sphingolipidoses and Allied Disorders, Plenum Press, New York, 1972, p. 77.

[27] T. Izumi, T. Ogawa, H. Koizumi, Y. Fukuyama, Normal developmental profiles of CSF gangliotetraose-series gangliosides from neonatal period to adolescence, Pediatr. Neurol. 9 (1993) 297—300.

[28] M. Trbojevic-Cepe, I. Kracun, Determination of gangliosides in human cerebrospinal fluid by high-performance thin-layer chromatography and direct densitometry, J. Clin. Chem. Clin. Biochem. 28 (1990) 863—872.

[29] M. Gisskn, L. Hagberg, G. Norkrans, A. Lekman, P. Fredman, Increased cerebrospinal fluid ganglioside GMI concentrations indicating neuronal involvement in all stages of HIV-1 infection, J. Neurovirol. 3 (1997) 148—152.

[30] K. Blennow, P. Davidsson, A. Wallin, P. Fredman, C.G. Gottfries, I. Karlsson, J.E. Månsson, L. Svennerholm, Gangliosides in cerebrospinal fluid in 'probable Alzheimer's disease, Arch. Neurol. 48 (1991) 1032—1035.

[31] E. Ginns, J. French, A. Fleischman, S. Cohen, GM1 ganglioside concentration in the cerebrospinal fluid of neonates and children, Pediatr. Res. 14 (1980) 1276—1277.

[32] A. Seyer, S. Boudah, S. Broudin, C. Junot, B. Colsch, Annotation of the human cerebrospinal fluid lipidome using high resolution mass spectrometry and a dedicated data processing workflow, Metabolomics 12 (2016) 91.

[33] A. Robu, C. Schiopu, F. Capitan, A.D. Zamfir, Mass spectrometry of gangliosides in extracranial tumors: application to adrenal neuroblastoma, Anal. Biochem. 509 (2016) 1—11.

[34] F. Capitan, A. Robu, L. Popescu, C. Flangea, Ž. Vukelić, A.D. Zamfir, B subunit monomers of cholera toxin bind G1 ganglioside class as revealed by chip-nanoelectrospray multistage mass spectrometry, J. Carbohydr. Chem. l34 (2015) 388—408.

[35] I. Cozma, M. Sarbu, C. Ilie, A.D. Zamfir, Structural analysis by electrospray ionization mass spectrometry of GT1 ganglioside fraction isolated from fetal brain, J. Carbohydr. Chem. 36 (2017) 247—264.

[36] M. Sarbu, A.D. Zamfir, Modern separation techniques coupled to high performance mass spectrometry for glycolipid analysis, Electrophoresis 39 (2018) 1155—1170.

[37] E. Sisu, C. Flangea, A. Serb, A. Rizzi, A.D. Zamfir, High-performance separation techniques hyphenated to mass spectrometry for ganglioside analysis, Electrophoresis 32 (2011) 1591—1609.

[38] A.D. Zamfir, Neurological analyses: focus on gangliosides and mass spectrometry, Adv. Exp. Med. Biol. 806 (2014) 153—204.

[39] R. Albulescu, A.J. Petrescu, M. Sarbu, A. Grigore, R. Ica, C.V.A. Munteanu, A. Albulescu, I.V. Militaru, A.D. Zamfir, S. Petrescu, C. Tanase, Mass Spectrometry for Cancer Biomarkers, IntechOpen, 2019, https://doi.org/10.5772/intechopen.85609.

[40] Y. Zhang, J. Wang, J. Liu, S. Han, S. Xiong, W. Yong, Z. Zhaoa, Combination of ESI and MALDI mass spectrometry for qualitative, semi-quantitative and in situ analysis of gangliosides in brain, Sci. Rep. 6 (2016) 25289.

[41] M. Sarbu, Z. Vukelic, D.E. Clemmer, A.D. Zamfir, Ion mobility mass spectrometry provides novel insights into the expression and structure of gangliosides in normal adult human hippocampus, Analyst 143 (2018) 5234—5246.

[42] M. Sarbu, A.C. Robu, R.M. Ghiulai, Ž. Vukelić, D.E. Clemmer, A.D. Zamfir, Electrospray ionization ion mobility mass spectrometry of human brain gangliosides, Anal. Chem. 88 (2016) 5166—5178.

[43] J. Gu, C.J. Tifft, S.J. Soldin, Simultaneous quantification of GM1 and GM2 gangliosides by isotope dilution tandem mass spectrometry, Clin. Biochem. 41 (2008) 413—417.

[44] H. Satoh, T. Yamauchi, M. Yamasaki, Y. Maede, A. Yabuki, H.S. Chang, T. Asanuma, O. Yamato, Rapid detection of GM1 ganglioside in cerebrospinal fluid in dogs with GM1 gangliosidosis using matrix-assisted laser desorption ionization time-of-flight mass spectrometry, J. Vet. Diagn. Investig. 23 (2011) 1202—1207.

[45] H.L. Gray-Edwards, X. Jiang, A.N. Randle, A.R. Taylor, T.L. Voss, A.K. Johnson, V.J. McCurdy, M. Sena-Esteves, D.S. Ory, D.R. Martin, Lipidomic evaluation of feline neurologic disease after AAV gene therapy, Mol Ther Methods Clin Dev 6 (2017) 135—142.

[46] H.L. Bernheimer, Zur kenntnis der ganglioside im liquor cerebrospinalis des menschen, Klin. Wochenschr. 47 (1969) 227—228.

[47] Y. Nagai, J.N. Kanfer, W.W. Tourtellotte, Preliminary observations of gangliosides of normal and multiple sclerosis cerebrospinal fluid, Neurology 23 (1973) 945—948.

[48] P. Davidsson, P. Fredman, L. Svennerholm, Gangliosides and sulfatide in human cerebrospinal fluid: quantitation with immunoaffinity techniques, J. Chromatogr. 496 (1989) 279—289.

[49] P. Davidsson, P. Fredman, J.E. Månsson, L. Svennerholm, Determination of gangliosides and sulfatide in human cerebrospinal fluid with a micro-immunoaffinity technique, Clin. Chim. Acta 197 (1991) 105—116.

[50] L. Svennerholm, P. Fredman, A procedure for the quantitative isolation of brain gangliosides, Biochim. Biophys. Acta 617 (1980) 97—109.

[51] Ž. Vukelić, W. Metelmann, J. Müthing, M. Kos, J. Peter-Katalinić, Anencephaly: structural characterization of gangliosides in defined brain regions, Biol. Chem. 382 (2001) 259—274.

[52] L. Svennerholm, Ganglioside designation, Adv. Exp. Med. Biol. 125 (1980) 11.

[53] IUPAC-IUB joint commission on biochemical nomenclature, Eur. J. Biochem. 257 (1998) 293—298.

[54] B. Domon, C.E. Costello, A systematic nomenclature of carbohydrate fragmentation in FAB-MS/MS spectra of glycoconjugates, Glycoconj. J. 5 (1988) 397—409.

[55] C.E. Costello, P. Juhasz, H. Perreault, New mass spectral approaches to ganglioside structure determination, Prog. Brain Res. 101 (1994) 45—61.

[56] Ž. Vukelić, S. Kalanj-Bognar, M. Froesch, L. Bîndila, B. Radić, M. Allen, J. Peter-Katalinić, A.D. Zamfir, Human gliosarcoma associated ganglioside composition is complex and distinctive as evidenced by high-performance mass spectrometric determination and structural characterization, Glycobiology 17 (2007) 504—515.

[57] C. Schiopu, C. Flangea, F. Capitan, A. Serb, Ž. Vukelić, S. Kalanj-Bognar, E. Sisu, M. Przybylski, A.D. Zamfir, Determination of ganglioside composition and structure in human brain hemangioma by chip-based nanoelectrospray ionisation tandem mass spectrometry, Anal. Bioanal. Chem. 395 (2009) 2465—2477.

[58] H.P. Schwarz, I. Kostyk, A. Marmolejo, C. Sarappa, Long-chain bases of brain and spinal cord of rabbits, J. Neurochem. 14 (1967) 91.

[59] A. Serb, C. Schiopu, C. Flangea, E. Sisu, A.D. Zamfir, Top-down glycolipidomics: fragmentation analysis of ganglioside oligosaccharide core and ceramide moiety by chip-nanoelectrospray collision-induced dissociation MS^2-MS^6, J. Mass Spectrom. 44 (2009) 1434—1442.

[60] P. Palestini, S. Sonnino, G. Tettamanti, Lack of the ganglioside molecular species containing the C20-long-chain bases in human, rat, mouse, rabbit, cat, dog, and chicken brains during prenatal life, J. Neurochem. 56 (1991) 2048.

[61] E. Sibille, O. Berdeaux, L. Martine, A.M. Bron, C.P. Creuzot-Garcher, Z. He, G. Thuret, L. Bretillon, E.A. Masson, Ganglioside profiling of the human retina: comparison with other ocular structures, brain and plasma reveals tissue specificities, PLoS One 11 (2016), e0168794.

[62] R.K. Yu, Y. Nakatani, M. Yanagisawa, The role of glycosphingolipid metabolism in the developing brain, J. Lipid Res. 50 (2009) S440.

[63] D. Fabris, M. Rožman, T. Sajko, Ž. Vukelić, Aberrant ganglioside composition in glioblastoma multiforme and peritumoral tissue: a mass spectrometry characterization, Biochimie 137 (2017) 56—68.

[64] C. Mosoarca, R.M. Ghiulai, C.R. Novaconi, Ž. Vukelić, A. Chiriac, A.D. Zamfir, Application of chip-based nanoelectrospray ion trap mass spectrometry to compositional and structural analysis of gangliosides in human fetal

cerebellum, Anal. Lett. 44 (2011) 1036—1049.

[65] A. Serb, C. Schiopu, C. Flangea, Z. Vukelić, E. Sisu, L. Zagrean, A.D. Zamfir, High-throughput analysis of gangliosides in defined regions of fetal brain by fully automated chip-based nanoelectrospray ionization multi-stage mass spectrometry, Eur. J. Mass Spectrom. 15 (2009) 541—553.

[66] A.F. Serb, E. Sisu, Z. Vukelić, A.D. Zamfir, Profiling and sequencing of gangliosides from human caudate nucleus by chip-nanoelectrospray mass spectrometry, J. Mass Spectrom. 47 (2012) 1561—1570.

[67] Sarbu M, Dehelean L, Munteanu CVA, Ica R, Petrescu AJ, Zamfir AD, Human caudate nucleus exhibits a highly complex ganglioside pattern as revealed by high-resolution multistage Orbitrap MS. J. Carbohydr. Chem.. DOI: 10.1080/07328303.2019.1669632

[68] S. Ando, N.C. Chang, R.K. Yu, High-performance thin-layer chromatography and densitometric determination of brain ganglioside compositions of several species, Anal. Biochem. 89 (1978) 437—450.